Eur Biophys J (2007) 36:1029–1037
DOI 10.1007/s00249-007-0208-5

ORIGINAL PAPER

Organization of reconstituted lipoprotein MexA onto supported lipid membrane

Sylvain Trépout · Jean-Christophe Taveau · Stéphane Mornet · Houssain Benabdelhak · Arnaud Ducruix · Olivier Lambert

Received: 14 February 2007 / Revised: 22 June 2007 / Accepted: 10 July 2007 / Published online: 31 July 2007

Abstract MexA, a periplasmic component of OprM-MexA-MexB tripartite multidrug efflux pump from *Pseudomonas aeruginosa*, is natively anchored via its fatty acid in the bacteria inner membrane protruding into the periplasm. We used supported lipid bilayer (SLB) to attach the protein to a single leaflet mimicking its perisplamic orientation. For that purpose, we studied the solubilization of DOPC lipid bilayer supported on silica surface with β-octyl glucoside (βOG). First we showed that SLBs resist to βOG concentrations that usually solubilize liposomes. Native form of MexA was directly inserted in the outer leaflet at (βOG concentrations in a range of 20–25 mM). Second, observations by cryo-electron microscopy (cryo-EM) revealed a dense protein layer attached to the surface corresponding to a 13-nm layer of MexA proteins. Analysis of protein densities allows proposing a schematic organization of native MexA inserted in lipid membrane. This structural organization provides further insights with respect to the partially solved structure of the soluble form.

Keywords Membrane protein · Multidrug resistance · Cryo-electron microscopy · Membrane protein on solid support · SLB · QCM-D

Presented at the joint biannual meeting of the SFB-GEIMM-GRIP, Anglet France, 14–19 October, 2006.

S. Trépout · J.-C. Taveau · S. Mornet · O. Lambert (✉)
Laboratoire d'Imagerie Moléculaire et Nano-Bio-Technologie, UMR 5248 CBMN, CNRS, Université Bordeaux 1, ENITAB, IECB, 2 rue Robert Escarpit, 33607 Pessac, France
e-mail: o.lambert@iecb.u-bordeaux.fr

H. Benabdelhak · A. Ducruix
Laboratoire de Cristallographie et RMN Biologiques, UMR 8015 CNRS, Faculté de Pharmacie, Université Paris Descartes, 4 avenue de l'observatoire, 75270 Paris Cedex 06, France

Present Address:
S. Mornet
European Commission Joint Research Centre Institute for Health and Consumer Protection, Via E. Fermi 1, TP 203, 21020 Ispra, Italy

Introduction

Pseudomonas aeruginosa is a Gram-negative bacterium that causes opportunistic infections in immuno-compromised patients and exhibits natural and acquired resistance to diverse antibiotics. Because of the broad spectrum of transported substances, these resistance systems are called multidrug efflux pumps. These pumps are tripartite complexes consisting of an energized inner membrane pump, a periplasmic adaptor or membrane fusion protein and an outer membrane channel protein. These special pump-systems form a transporter unit bridging both the inner and the outer membrane and are largely widespread among the Gram-negative bacteria (Andersen 2003). The most extensively characterized systems are MexAB-OprM from *P. aeruginosa* and the AcrAB/TolC homologue system from *E. coli*.

The inner membrane protein AcrB of *E. coli* was the first crystallized proton antiporter belonging to the resistance nodulation cell division family (Murakami et al. 2002). It comprises a homotrimer of about 110 kDa per monomer. Each subunit contains 12 transmembrane helices forming the 40-Å-thick transmembrane region and a huge domain protruding 70 Å into the periplasm. Murakami and co-workers have recently proposed that the drug transport occurs in a three-step rotating mechanism in which each protomer captures drugs from the periplasm and exports

them in a cyclic conformation change up to the central pore induced by the trimeric assembly (Murakami et al. 2002, 2006). This was supported by the recent publication of the crystal structure of asymmetric AcrB (Sennhauser et al. 2007).

The outer membrane components OprM and the homologue TolC of *E. coli* are also homotrimers forming a cylindrical channel (Koronakis et al. 2000; Akama et al. 2004a; Lambert et al. 2005). The trimers are composed of 12-stranded β-barrel inserted in the outer membrane and of a 100-Å-long α-helical barrel extended into the periplasmic space. Recently, a direct interaction between the rim of the AcrB funnel and the periplasmic end of TolC could be detected by site-directed disulfide cross-linking suggesting a possible passage of exported compounds from the transporter into the channel (Tamura et al. 2005).

For the assembly of a functional efflux pump, a third component—the periplasmic adaptor protein—named MexA, is also essential (Fralick 1996). The latter is a non-transmembrane protein that behaves as a hydrophobic protein because its fatty acid anchor thus needs detergent for its solubilization. The partial structure of MexA without its fatty acid moiety has been determined (Akama et al. 2004b; Higgins et al. 2004). MexA monomers show a 47-Å-long α-helical hairpin domain connected to a flattened β-sandwich domain and a third $\alpha + \beta$ domain made of a six-stranded β-barrel with a short α-helix. However, a large part composed of 28 N-terminal and 101 C-terminal residues—representing one third of the protein—could not be solved (Akama et al. 2004b; Higgins et al. 2004). Whereas the inner and outer membrane proteins were crystallized in a trimeric state, MexA crystallized as a tri-decamer. More precisely, it assembles in two horseshoes containing either six or seven monomers superimposed in a sandwich. Recently, a second representative adaptor protein AcrA from *E. coli* strongly resembling MexA packs as an apparent dimer of dimers (Mikolosko et al. 2006). A complementary approach consists in the study of native form of MexA protein anchored into lipid membrane.

Biomimetic systems are very useful to understand the protein–protein assembly and protein–lipid interactions. Insertion of membrane proteins into artificial membrane after detergent removal is a widely used method for transmembrane protein (Rigaud et al. 1995). However, for proteins anchored to the membrane surface by a post-synthetic modification, such as myristoylation, farnesylation or GPI-linkages, the reconstitution process is less documented. As the lipid anchor usually needs detergent for its solubilization, a first approach is based on the reconstitution process from mixed micelles lipid/detergent followed by detergent depletion (Lehto and Sharom 1998; Reid-Taylor et al. 1999; Sharom and Letho 2002). A second approach consists in a direct incorporation into preformed liposomes in the presence of detergent to promote protein insertion (Angrand et al. 1997; Ronzon et al. 2004). The advantage of the latter strategy is the unidirectional orientation of the protein in the membrane, although a limited range of detergent concentration is permitted since liposomes need to be destabilized for protein binding, but not solubilized by an excess of detergent. In addition to these vesicular approaches, strategies involving planar substrates have been recently developed for studying synthetic lipoproteins on supported lipid bilayers (SLB) using either direct incorporation without detergent or proteoliposome deposition (Bader et al. 2000, Grogan et al. 2005). Nowadays the use of solid supports is of particular interest because the protein controlled-orientation can be driven by engineered surfaces (Salafsky et al. 1996, Ataka et al. 2004). In this context we have recently studied the formation of supported lipid bilayers on silica nanoparticles (nano/SLBs) and the reconstitution of membrane protein selectively oriented on positively-charged nanoparticles (Mornet et al. 2005; Trépout et al. 2007).

In the present study, we describe a rapid procedure of MexA reconstitution on nano/SLBs amenable to structural and biophysical studies. After characterizing the influence of detergent on SLB, MexA proteins solubilized in the presence of detergent were directly inserted into a SLB via their fatty acid. Thus, we report on the architecture of wild-type MexA subunits anchored in the distal leaflet of SLB using cryo-electron microscopy (cryo-EM).

Materials and methods

Materials and reagents

Dioleolylphosphatidylcholine (DOPC), Octyl-βD-Glucopyranoside (βOG) and Tetraethoxysilane (TEOS) were, respectively, purchased from Avanti Polar Lipids (USA), from Sigma, and from Aldrich.

Preparation of MexA proteins

MexA from *P. aeruginosa* was cloned in a pBAD33 plasmid in *E. coli* (Guzman et al. 1995). The MexA lipoprotein expression and purification was performed according to Yoneyama et al. (2000) and adapted using the following protocol. The membrane envelopes from broken *E. coli* cells were solubilized in 20 mM Tris–HCl pH 8, 10% glycerol, 15 mM imidazole, 50 mM βOG overnight at 20°C. The solubilized membrane proteins were loaded onto a Ni-NTA resin column and then were eluted with a linear gradient of imidazole (60–500 mM). The fractions containing MexA proteins were pooled and concentrated

to 5 mg/ml. Finally, mature lipoproteins MexA were exchanged for suitable buffer by dialysis in the presence of 20 mM Tris–HCl pH 8.0, 200 mM NaCl, 10% glycerol and 20 mM βOG.

Preparation of unilamellar vesicles

Lipids were dissolved in chloroform, dried under a stream of nitrogen and then in a vacuum desiccator overnight. Unilamellar vesicles were prepared by reverse-phase evaporation, followed by sequential extrusion through 0.4, 0.2 and 0.1 μm Nucleopore filters (Paternostre et al. 1988). Small unilamellar vesicles (SUVs) were obtained by sonication with a tip sonicator as described previously (Richter et al. 2003).

Preparation of silica nanoparticles

Colloïdal silica nanoparticles were prepared as previously described (Mornet et al. 2005). TEOS was mixed with a dry ethanol solution containing ammonia and were stirred overnight. Silica sol was prepared by evaporation of ammonia and ethanol and dialyzed against ultrapure water (10 MΩ) and stored at room temperature. Before use, silica nanoparticles were diluted to a concentration of 1 g/l in 10 mM Hepes buffer at pH 7.4.

NanoSLB formation and detergent solubilization

DOPC liposomes (150 μg/ml) were deposited on silica nanoparticles (50 μg/ml) in 150 mM NaCl, 10 mM Hepes pH 7.4 inducing the formation of supported lipid bilayers on nanoparticles (nano/SLB). For solubilization experiments, an equivalent volume of solution containing the detergent was added. The sample was observed after 1 h of incubation time.

Reconstitution of MexA protein on nanoparticles

Nano/SLBs were formed by mixing a solution containing DOPC SUVs at 30 μg/ml with a solution of silica nanoparticles at a concentration of 20 μg/ml. The nano/SLB solution was mixed with an equivalent volume of buffer solution containing the final desired βOG concentration. Then MexA solution (1 μg/ml) containing the same βOG concentration was added. After 1 h of incubation time, the detergent was removed with polystyrene beads (SM2 Biobeads, Biorad) according to Rigaud et al. (1997).

Cryo-electron microscopy and image analysis

A 5-μL sample was deposited onto a holey carbon coated copper grid. The excess was blotted with a filter paper. Unstained samples were frozen into liquid ethane and the grids were mounted onto a Gatan 626 cryoholder, transferred into the microscope, and kept at a temperature of about –175°C. Sample observations were performed with a Tecnai F20 FEI transmission electron microscope, operating at 200 kV. Low-dose images were recorded at a nominal magnification of ×50,000 with a 2k × 2k USC1000 slow-scan CCD camera (Gatan, CA, USA). Radial profile plots were calculated on inverted contrast images using plug-in "Radial Profile Extended" of Image J (Rasband 1997) by averaging densities over various angular ranges.

Quartz crystal microbalance with dissipation Monitoring

The procedure of cleaning untreated silica-coated sensor was described previously (Richter et al. 2003). QCM-D measurements were performed with the Q-SENSE D300 system equipped with an Axial Flow Chamber (QAFC 302). Upon interaction of (soft) matter with the surface of a sensor crystal, changes in the resonance frequency, f, related to attached mass (including coupled water), and in the dissipation, D, related to frictional (viscous) losses in the adlayer were measured with a time resolution of better than 1 s. Measurements were performed in exchange mode which allows following processes of adsorption and surface adlayer changes in situ, while sequentially exposing different solutions to the supports. Resonance frequency and dissipation were measured at several harmonics (15, 25, 35 MHz) simultaneously. The working temperature was 24°C. Changes in dissipation and in normalized frequency ($\Delta f = \Delta f_n/n$, with n being the overtone number) of the third overtone ($n = 3$, i.e., 15 MHz) are presented. Adsorbed masses, Δm, are calculated according to the Sauerbrey equation, $\Delta m = -C\Delta f$, with the mass sensitivity constant $C = 17.7$ ng cm^{-2} Hz^{-1} for 5 MHz sensor crystals.

Results and discussion

In the present paper, our aim was the structural study of the wild-type MexA protein anchored in lipid bilayer, while previous structural studies were carried out on soluble form. In order to control the protein insertion into one leaflet as occurring in bacteria, we propose the use of SLB to mimic the leaflet accessibility (Fig. 1). Indeed the deposition of liposome on silica surface either on planar surface or on nanoparticles lead to the formation of a continuous supported lipid bilayer that was well characterized by QCM-D and cryo-EM, respectively (Richter

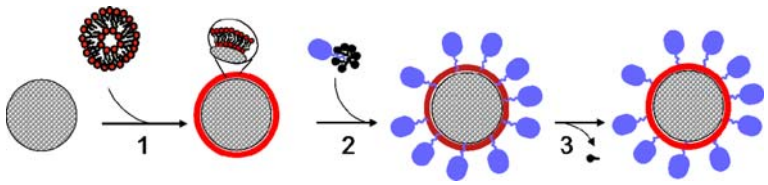

Fig. 1 Scheme of MexA binding to nano/SLBs. Nano/SLB is formed on silica nanoparticles via a liposome decomposition process (*step1*). MexA proteins purified in the presence of βOG are attached to nano/SLB via their fatty acid (*step2*). After detergent removal MexA inserted into the outer leaflet has a unique orientation (*step3*)

et al. 2003; Richter and Brisson 2004; Mornet et al. 2005). So the distal leaflet of supported lipid bilayer facing the solvent is only accessible to MexA proteins, the proximal leaflet being in close contact with the silica surface. Since the wild-type MexA protein was purified in the presence of 20 mM βOG, the binding of MexA onto nano/SLBs was carried out in three main steps: (1) nano/SLB formation, (2) binding of MexA proteins via its fatty acid and (3) detergent removal (Fig. 1). MexA binding was studied on two complementary supports, planar sensors and nanoparticles and was characterized by QCM-D and cryo-EM.

In the second part of the results, we analyzed the structural organization of wild-type MexA protein bound to lipid membrane by cryoEM. The incorporation of MexA in the outer leaflet gave access to the side view revealing the protein/membrane distance and allowing the localization of the disordered domain described in the X-ray crystallography studies.

Effect of βOG on SLB monitored with QCM-D

The solubilization process of SLB by detergent was studied by QCM-D. The DOPC vesicles were injected at t = 360 s (6 min) and their interactions with the silica support triggered the SLB formation few minutes after injection (Fig. 2). The final frequency shift of –25 ± 2 Hz and the low dissipation of 0.5×10^{-6} corresponded to the formation of a lipid bilayer covering the support with minor defects as previously described in the literature (Keller and Kasemo 1998; Richter et al. 2003). At t = 1,560 s (26 min) then the detergent solution was injected and rinsed at t = 2,700 (46 min). Before rinsing, since the presence of detergent affected the variation of frequency due to a buffer effect, the mass release could not be directly readable. After rinsing with buffer without detergent, the variation of frequency reflected directly the loss of mass. The absorbed mass of SLB did not change after injection of 10 and 15 mM βOG, respectively. A 20-mM βOG injection induced a mass loss of 8 Hz corresponding to an apparent loss of 30% SLB. The solubilization of the SLB appeared more effective at 25 and 30 mM βOG with a residual mass of 8 and 6 Hz, respectively.

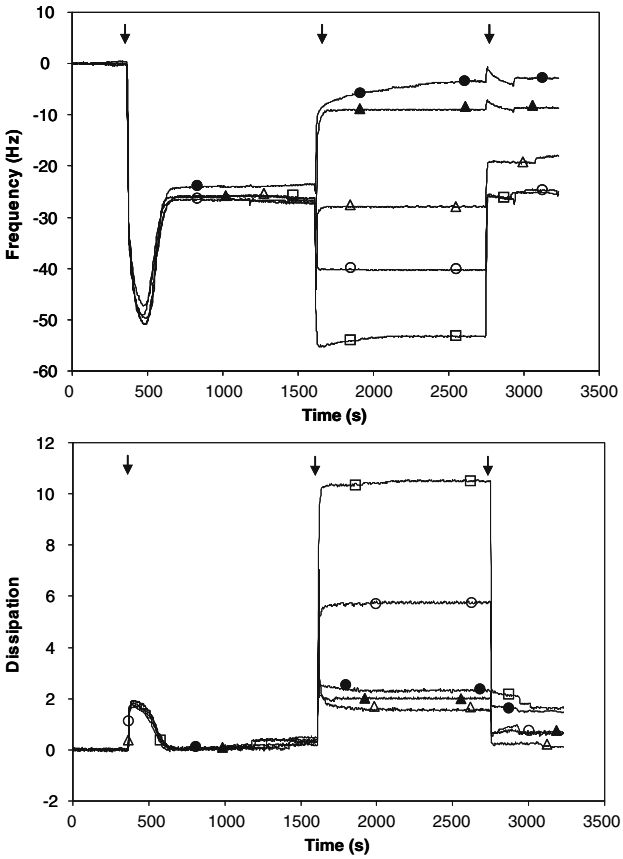

Fig. 2 QCM-D response for the formation of SLB and for detergent effect on SLB. Change in frequency ΔF and in dissipation ΔD on silica surface. For each experiment, DOPC vesicles injected at 300 s were decomposed into a SLB corresponding to a frequency shift of –25 Hz and then βOG solution was added at 1,600 s and rinsed with buffer at 2,600 s. Measurements have been performed for 10 mM (*open circle*), 15 mM (*open square*), 20 mM (*open triangle*), 25 mM (*filled triangle*), 30 mM βOG (*filled circle*), respectively. The final frequency shift indicates the residual mass adsorbed on the support

Solubilization of nano/SLB with βOG

To visualize the SLB in the presence of detergent, we have studied by cryo-EM the solubilization of nano/SLB. Silica nanoparticles were mixed with DOPC vesicles in order to form the nano/SLBs. After 15 min of incubation, βOG was added at various final concentrations of 10, 15, 20, 25 and

30 mM. The mixtures were observed by cryo-EM (Fig. 3). Silica nanoparticles appeared as dense spheres of about 110 nm in diameter. SLB formed at the particle surface produced an extra dark line (black arrows) corresponding to the distal leaflet of SLB as previously described (Mornet et al. 2005). For comparison, bare silica nanoparticles are shown in the insert of Fig. 3a. Since the formation of nano/SLBs is performed with an excess of lipid vesicles, vesicles were visible in the neighborhood of the nano/SLBs (asterisk in Fig. 3a). Then it was possible to follow the solubilization process of both vesicles and nano/SLBs for increasing βOG concentration. On the one hand vesicles were visible up to 15 mM βOG (insert of Fig. 3c) although their number decreases. At 20 mM βOG no more vesicles were observed, due to their solubilization (insert in Fig. 3d). On the other hand, nano/SLBs looked similar to those in the absence of detergent even in the presence of 20 mM βOG (Fig. 3d). In the presence of 25 mM βOG, the dark line around the particles became faint, showing that the nano/SLBs were destabilized by βOG (Fig. 3e). At 30 mM βOG, nano/SLBs disappeared (Fig. 3f).

For liposome suspension, the solubilization process of vesicles can be described by the Eq. (1) (Silvius 1992; Rigaud et al. 1995):

$$D_{\text{tot}} = D_{\text{w}} + R_{\text{sol}}\,[\text{lip}] \qquad (1)$$

where D_{tot} and [lip] are the total detergent and lipid concentrations; D_{w} is the aqueous detergent concentration; R_{sol} is the detergent to lipid ratio in mixed micelles, i.e. the ratio at which the lamellar to micellar transition finishes. For βOG, R_{sol} = 2.6 mol/mol and D_{w} = 17 mM (Rigaud et al. 1995).

For the lipid concentration corresponding to our system (i.e. [lip] = 0.2 mM), the total solubilization should occur at 17–18 mM βOG. In addition, Nosjean and Roux (2003) have studied the solubilization process by measuring the turbidity at various βOG concentrations. They showed a total solubilization of a 0.25-mg/ml phosphatidylcholine liposome suspension at 20 mM βOG. These data perfectly support our cryoEM results showing the solubilization of liposomes at 20 mM βOG.

Moreover, as shown by cryoEM and QCM-D results, SLBs are not removed from the surface in the presence of 20 mM βOG indicating a less sensitivity to βOG than vesicles. The liposomes are fully solubilized at 20 mM βOG (inset in Fig. 3d) but for SLBs, the complete solubilization occurs at a higher βOG concentration (i.e. 25–30 mM) as evidenced by QCM-D (Fig. 2) and by cryo-EM (Fig. 3e–f). Silica support slightly changes the solubilization threshold of lipid bilayer. It is known that βOG monomers penetrate the membrane and form mixed detergent–lipid bilayer throughout a half-sided incorporation and a fast flip–flop leading to a symmetric partitioning (Keller et al., 1997; leMaire et al., 1987; Wenk et al., 1997). SLBs are slightly different from vesicles because of the interaction of the proximal leaflet with the silica support. Lateral diffusion of lipid in the proximal leaflet is

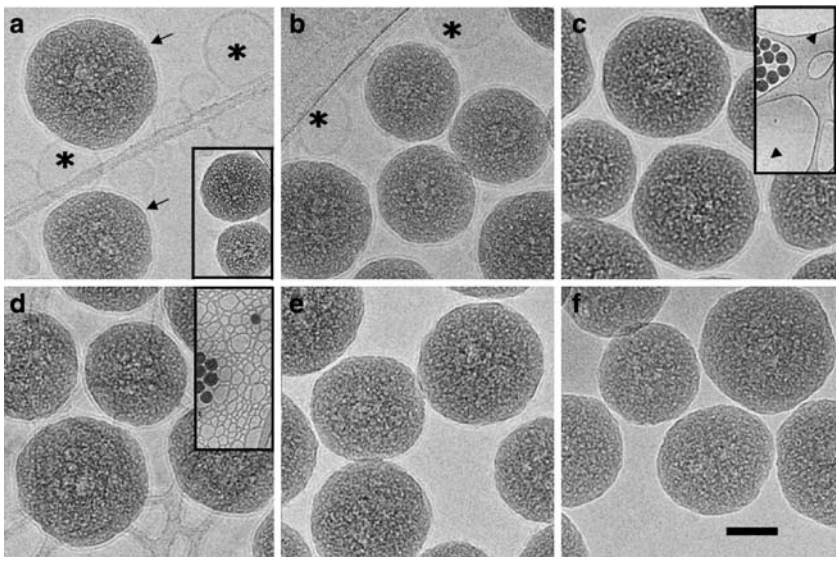

Fig. 3 CryoEM of nano/SLBs incubated in the presence of 0, 10, 15, 20, 25 and 30 mM βOG, respectively (a-f). **a** Annular densities around the silica nanoparticles correspond to nano/SLBs (*black arrows*). Inset 110 nm bare nanoparticles. **b**, **c** At 10 and 15 mM βOG, nano/SLBs were clearly observed as well as vesicles (*asterisk*) even at 15 mM βOG (see *arrowheads* in *inset* in **c**). **d** At 20 mM βOG, SLBs remained visible while liposomes have disappeared (*inset*). **e** At 25 mM βOG, faint densities were present at the silica surface. **f** At 30 mM βOG, nano/SLBs were solubilized. (scale bar 50 nm). Insets in **a**, **c**, and **d** show low magnification views

slower than in the distal leaflet exposed to the solution (Hetzer et al. 1998). Thus the reduced mobility of the proximal leaflet could have a direct effect on detergent incorporation by limiting or slowing down the flip–flop process.

Thanks to the peculiar behavior of SLB, the approach based on direct insertion of lipoproteins into lipid membrane can be extended to SLBs since they resist to higher βOG concentrations than vesicles. Therefore this method has been performed for MexA proteins purified at 20 mM βOG (as mentioned in "Materials and methods" section).

Binding of MexA to SLB and nano/SLB studied at various detergent concentrations

Adsorptions of a 30 μg/ml MexA solution on SLBs in the presence of 20, 25, and 30 mM βOG were followed by QCM-D (Fig. 4). After protein injection, a mass was adsorbed rapidly to the SLB and has reached a plateau in these three experimental conditions. After 1 h of incubation time, the chamber was rinsed with buffer without detergent. A decrease of dissipation curves was observed—mainly due to a buffer effect—then the final frequency and dissipation values were respectively ΔF = –76 Hz, $\Delta D = 2 \times 10^{-6}$; ΔF = –67 Hz, $\Delta D = 1 \times 10^{-6}$ and ΔF = –76 Hz, $\Delta D = 2.5 \times 10^{-6}$. The difference in mass deposition and dissipation values could reflect various MexA deposition pathways. Moreover, MexA did not bind to SLB when the solution was injected in the absence of detergent.

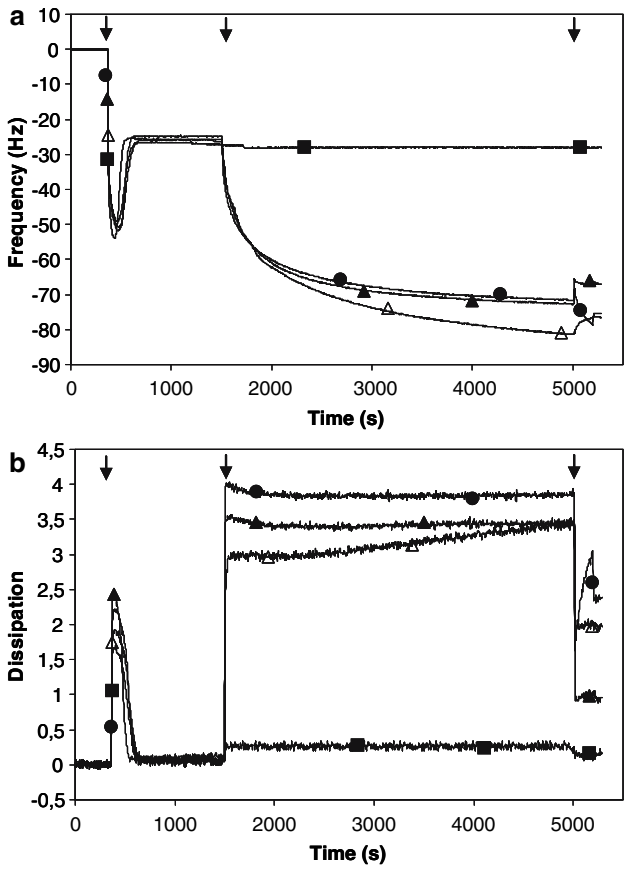

Fig. 4 QCM-D response for the binding of MexA on silica surface with, 0, 20, 25, and 30 mM βOG. **a** Change in frequency ΔF of MexA binding on DOPC SLB. **b** Change in dissipation ΔD. From left to right, *arrows* indicate (i) injection of liposomes, (ii) injection of MexA, (iii) a rinse with buffer without detergent. Measurements have been performed for 0 mM (*filled square*), 20 mM (*open triangle*), 25 mM (*filled triangle*), 30 mM βOG (*filled circle*), respectively

Native MexA is a lipoprotein that contains a palmitoyl chain linked on the N-terminal cysteine residue and requires detergent to solubilize the lipid moiety. Moreover, from the literature (Akama et al. 2004b), mutant MexA with deleted fatty acid are soluble proteins meaning that the protein moiety does not behave as a transmembrane protein. The fact that no adsorption of MexA on SLB was measured by QCM-D in the absence of detergent indicates that the protein moiety itself does not interact with the lipid bilayer.

In the presence of 30 mM βOG, MexA proteins are adsorbed on silica surface in a non-specific way since the SLB is solubilized as shown in Fig. 2. And at 20 mM βOG, SLB is still present on silica surface, covering at least 70% of the surface. Thus MexA binds (1) to SLB via MexA lipid anchor or (2) to silica surface through SLB defects or (3) to a mixture of both. However, a similar amount of MexA is adsorbed on the sensor whatever the detergent concentration (Fig. 4), meaning that MexA covers SLB or silica surface with a comparable density. Therefore we can conclude that there is a MexA/SLB interaction likely mediated by fatty acid even though we could not quantify the ratio of MexA bound to SLB with respect to its adsorption on silica surface at 20 mM βOG.

Since MexA is able to bind to planar SLB in the presence of βOG, structural characterization of native MexA attached to lipid bilayer was carried out on nanoparticles covered by SLB. Such assemblies are suitable for cryo-EM technique because they reveal the side view of protein interacting with the lipid bilayer.

First, nano/SLBs were produced by DOPC vesicle decomposition on silica nanoparticles, then MexA proteins were added (Fig. 5). Cryo-EM images of the mixture showed dense particles of silica nanoparticles surrounded by rod-like structures (white arrows) corresponding to MexA proteins (Fig. 5a, b). The protein binding was successful for βOG concentrations in a range of 20–25 mM while only nano/SLBs were observed at lower βOG concentrations (data not shown). After detergent removal with polystyrene beads, the protein layer was preserved and the reconstituted lipid bilayer was revealed by the fine layer of electron dense material close to the particle (black arrows

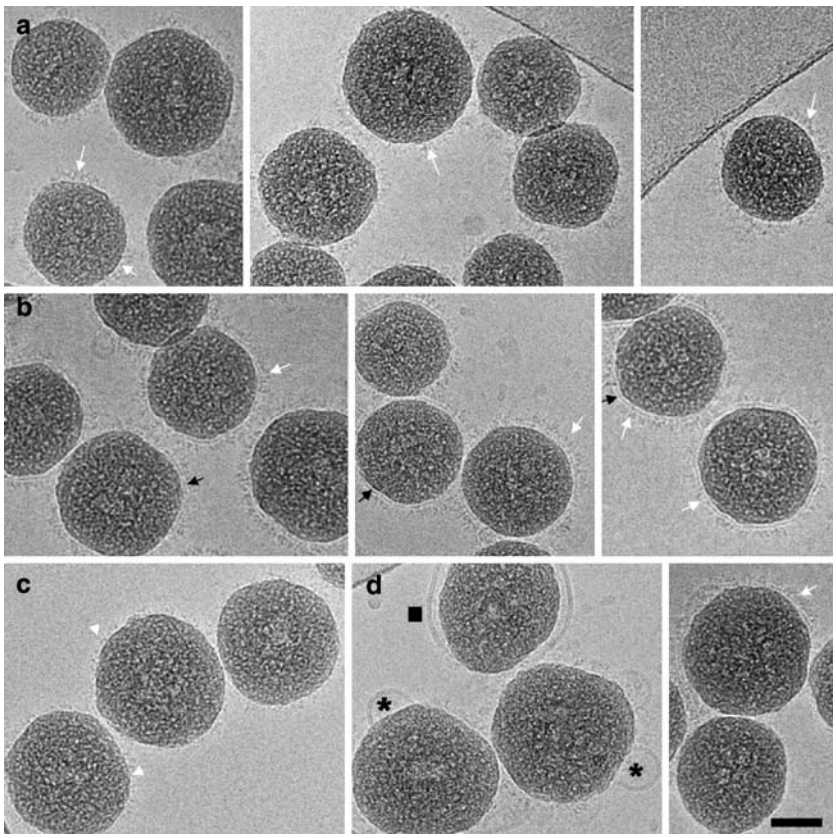

Fig. 5 Cryo-EM images of MexA inserted into nano/SLBs. **a** Fields of view of nano/SLBs mixed with MexA in the presence of 25 mM βOG. MexA proteins were clearly visible at nanoparticle surface (*white arrows*). **b** Fields of view of dense layers of MexA molecules reconstituted into SLBs (*black arrows*) after detergent removal. **c**, **d** In the presence of 30 mM βOG, MexA proteins were adsorbed (*white arrow heads* in **c**). After detergent removal, silica nanoparticles were covered irregularly with proteoliposomes (*asterisks*) and membrane-reconstituted MexA facing to silica surface (*black square*) and to the solvent (*white arrow*) (**d**). Scale bar 50 nm

in Fig. 5b). Above 25 mM βOG, protein adsorption was observed on silica surface (white arrow heads Fig. 5c). However, after detergent depletion, reconstituted proteoliposomes and MexA-containing membranes appeared randomly attached to silica surfaces (Fig. 5d). Moreover, MexA proteins were oriented facing to the solvent (white arrow) or to the silica surface (black square). In conclusion, supported lipid bilayers must be destabilized but not solubilized by βOG to insert MexA molecules in a unidirectional orientation.

The presence and size of rods suggest that MexA proteins formed a multimeric architecture anchored in the lipid bilayer although the degree of oligomerization is unknown. Radial profile plots were calculated for various nano/SLBs exhibiting MexA proteins. A typical profile is presented in Fig. 6a and for the sake of clarity, the image contrast was inverted so that resulting peaks from biological densities are above the background. This graph is centered on peak L that corresponds to the distal leaflet of the SLB. The left part of the profile shows the silica densities ending by a large peak (named S in Fig. 6a) including a shoulder likely revealing the proximal leaflet in close contact with the silica bead. Three successive peaks (respectively, noted P1, P2, and P3) visible along the profile depict the densities of the rod-like structures. Their distances from peak L are 4, 8, and 13 nm, respectively. Therefore, at the present resolution the overall structure of MexA protein on nano/SLBs can be estimated to 13 nm long and appears as three areas of high densities as summarized in the scheme of Fig. 6b. This distance is larger compared to the length of 9 nm given by the atomic model (Akama et al. 2004; Higgins et al. 2004). However, this atomic model should be considered as partial due to a "disordered" and unsolved domain composed of 28 residues of the N terminus and 101 residues of the C terminus. Therefore, the difference in size of 4 nm between our data and the atomic model could correspond to an estimation of the "disordered" domain size. Moreover the latter is presumed to be in contact with the lipid bilayer through the lipid attachment anchor meaning that it would likely be included in the peak P1 (hatched grey area in Fig. 6b). The dimension of this "disordered" domain is compatible with the distance of the 28 N-terminal residues bridging the gap between the solved domains and the lipid attachment. It is tempting to extrapolate from the width of the three peaks the distribution of the four domains: P1 could correspond to "disordered" domains and to α-helical hairpin domains, P2 to β-sandwich domains and P3 to $\alpha + \beta$ domains.

We were able to deposit a 13-nm thick monolayer of MexA protein linked to SLB as characterized by cryo-EM and QCM-D techniques. In the light of these results, our previous experiment of MexA/OprM interaction (Trépout

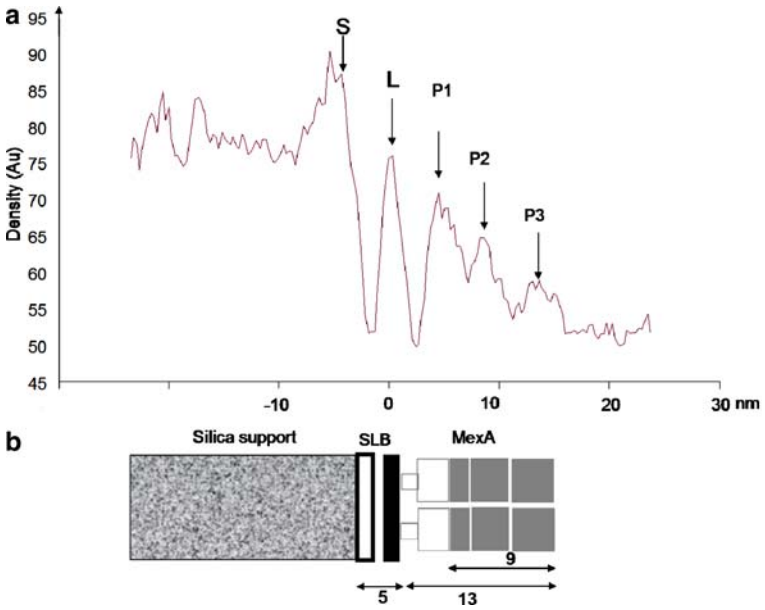

Fig. 6 Radial profile plot of nano/SLB exhibiting MexA proteins. a The profile is centered on the density peak of the distal leaflet of SLB (L), the peak (S) corresponding to the particle edge. From L, three peaks of protein density (P1, P2 and P3) are observed at 4, 8 and 13 nm respectively. **b** Schematic model of MexA on SLB composed of the silica particle (granite texture), SLB (*white* and *black rectangles*) for which only the distal leaflet is visible and MexA (*gray rectangle*). The protein moiety, which is the closest to the distal leaflet (*open rectangle*) may correspond to the anchor and the domain unsolved in the atomic model. 5, 13 and 9 nm correspond respectively to the distances of lipid bilayer, the overall protein size and the length given by the X-ray atomic model

et al. 2007) could correspond to the binding of MexA monolayer on top of OprM layer oriented on aminated support. Indeed, the 95 Hz additional mass of MexA bound to OprM measured in Trépout et al. (2007) is compatible with a single layer of MexA proteins corresponding to about 76 Hz according to our present data. Moreover the authors showed that OprM molecules are organized in a densely packed layer, exposing their 10-nm long periplasmic helices to the solvent. Thus the mass adsorption of MexA proteins was mainly mediated by protein–protein interactions and unlikely by protein–lipid bilayer interaction because it was hardly accessible to MexA.

In a structural context, the architecture of native MexA bound to lipid membrane observed in our experimental conditions cannot be related to the X-ray crystalline form where mutant MexA proteins are arranged in two multimeric funnel-like structures packed head-to-head leading to an overall size of 21 nm (Akama et al. 2004b; Higgins et al. 2004). The fact that we found approximately half the height of the X-ray assembly, suggests that native MexA protein is likely arranged in a single funnel on top of the lipid bilayer.

Conclusion

We show here that DOPC SLBs on silica are more detergent-resistant than pure DOPC liposomes. Binding of MexA lipoproteins was achieved in the distal leaflet of SLB leading to a unidirectional orientation. Cryo-EM study reveals a dense protein layer attached to the surface corresponding to a 13-nm layer of MexA proteins. In these experimental conditions, MexA arrangement and orientation with respect to lipid bilayer are favorable for a structural study of OprM / MexA complexes as previously measured by QCM-D (Trépout et al. 2007) by 3D imaging techniques like cryoelectron tomography that do not require sample crystallization.

Acknowledgment This work has been supported in part by EC grants "NMP4-CT2003-505868- Nanocues", EC grants "QLR-2000-01339" and program ACI "Dynamique et réactivité des assemblages biologiques" DRAB04/136. The authors wish to thank Xavier Moreel, Dimitri Lerouge and Joséphine Lai Kee Him for technical assistance with MexA and QCM-D. Sylvain Trépout is a recipient of a PhD fellowship of French Ministry of Education and Research and Technology (MENRT).

References

Akama H, Kanemaki M, Yoshimura M, Tsukihara T, Kashiwagi T, Yoneyama H, Narita S, Nakagawa A, Nakae T (2004a) Crystal structure of the drug discharge outer membrane protein, OprM, of *Pseudomonas aeruginosa*: dual modes of membrane anchoring and occluded cavity end. J Biol Chem 279:52816–52819

Akama H, Matsuura T, Kashiwagi S, Yoneyama H, Narita S, Tsukihara T, Nakagawa A, Nakae T (2004b) Crystal structure of the membrane fusion protein, MexA, of the multidrug transporter in *Pseudomonas aeruginosa*. J Biol Chem 279:25939–25942

Andersen C, (2003) Channel-tunnels: outer membrane components of type I secretion systems and multidrug efflux pumps of Gram-negative bacteria. Rev Physiol Biochem Pharmacol 147:122–165

Angrand M, Briolay A, Ronzon F, Roux B (1997) Detergent-mediated reconstitution of a glycosyl-phosphatidylinositolprotein into liposomes. Eur J Biochem 250:168–176

Ataka K, Giess F, Knoll W, Haber-Pohlmeier S, Richter B, Heberle J (2004) Oriented attachment and membrane reconstitution of His-tagged cytochrome c oxidase to a gold electrode: in situ monitoring by surface-enhanced infrared absorption spectroscopy. J Am Chem Soc 126:16199–16206

Bader B, Kuhn K, Owen DJ, Waldmann H, Wittinghofer A, Kuhlmann J (2000) Bioorganic synthesis of lipid-modified proteins for the study of signal transduction. Nature 403:223–226

Fralick JA (1996) Evidence that TolC is required for functioning of the Mar/AcrAB efflux pump of *Escherichia coli*. J Bacteriol 178:5803–5805

Grogan MJ, Kaizuka Y, Conrad RM, Groves JT, Bertozzi CR (2005) Synthesis of lipidated green fluorescent protein and its incorporation in supported lipid bilayers. J Am Chem Soc 127:14383–14387

Guzman LM, Belin D, Carson MJ, Beckwith J (1995) Tight regulation, modulation, and high-level expression by vectors containing the arabinose PBAD promoter. J Bacteriol 177:4121–4130

Higgins MK, Bokma E, Koronakis E, Hughes C, Koronakis V (2004) Structure of the periplasmic component of a bacterial drug efflux pump. Proc Natl Acad Sci USA 101:9994–9999

Hetzer M, Heinz S, Grage S, Bayerl TM (1998) Asymmetric molecular friction in supported phospholipid bilayers revealed by NMR measurements of lipid diffusion. Langmuir 14:982–984

Keller CA, Kasemo K (1998) Surface specific kinetics of lipid vesicle adsorption measured with a quartz crystal microbalance. Biophys J 75:1397–1402

Keller M, Kerth A, Blume A (1997) Thermodynamics of interaction of octyl glucoside with phosphatidylcholine vesicles: partitioning and solubilization as studied by high sensitivity titration calorimetry. Biochim Biophys Acta 1326:178–192

Koronakis V, Sharff A, Koronakis E, Luisi B, Hughes C (2000) Crystal structure of the bacterial embrane protein TolC central to multidrug efflux and protein export. Nature 405:914–919

Lambert O, Benabdelhak H, Chami M, Jouan L, Nouaille E, Ducruix A, Brisson A (2005) Trimeric structure of OprN and OprM efflux proteins from *Pseudomonas aeruginosa*, by 2D electron crystallography. J Struct Biol 150:50–57

Lehto MT, Sharom FJ (1998) Release of the glycosylphosphatidylinositol-anchored enzyme ecto-5'-nucleotidase by phospholipase C: catalytic activation and modulation by the lipid bilayer. Biochem J 332:101–109

leMaire M, Moller JV, Champeil P (1987) Binding of a non-ionic detergent to membranes: flip–flop rate and location on the bilayer. Biochemistry 26:4803–4810

Mikolosko J, Bobyk K, Zgurskaya HI, Ghosh P (2006) Conformational flexibility in the multidrug efflux system protein AcrA. Structure 14:577–587

Mornet S, Lambert O, Duguet E, Brisson A (2005) The formation of supported lipid bilayers on silica nanoparticles revealed by Cryoelectron microscopy. Nano Lett 5:281–285

Murakami S, Nakashima R, Yamashita E, Yamaguchi A (2002) Crystal structure of bacterial multidrug efflux transporter AcrB. Nature 419:587–593

Murakami S, Nakashima R, Yamashita E, Matsumoto T, Yamaguchi A (2006) Crystal structures of a multidrug transporter reveal a functionally rotating mechanism. Nature 443:173–179

Nosjean S, Roux B (2003) Anchoring of glycosylphosphatidylinosiyol-proteins to liposomes. Methods Enzymol 12:216–232

Paternostre MT, Roux M, Rigaud JL (1988) Mechanisms of membrane protein insertion into liposomes during reconstitution procedures involving the use of detergents. 1. Solubilization of large unilamellar liposomes (prepared by reverse-phase evaporation) by triton X-100, octyl glucoside, and sodium cholate. Biochemistry 27:2668–2677

Rasband WS 1997–2005 ImageJ U. S. National Institutes of Health, Bethesda, http://www.rsb.info.nih.gov/ij/

Reid-Taylor KL, Chu JWK, Sharom FJ (1999) Reconstitution of the glycosylphosphatidylinositol-anchored protein Thy-1: interaction with membrane phospholipids and galactosylceramide. Biochem Cell Biol 77:189–200

Richter R, Brisson A (2004) QCM-D on mica for parallel QCM-D-AFM studies. Langmuir 20:4609–4613

Richter R, Mukhopadhay A, Brisson A (2003) Pathways of lipid vesicle deposition on solid surfaces: a combined QCM-D and AFM study. Biophys J 85:3035–3047

Rigaud JL, Pitard B, Levy D (1995) Reconstitution of membrane proteins into liposomes: application to energy-transducing membrane proteins. Biochim Biophys Acta 1231:223–246

Rigaud JL, Mosser G, Lacapere JJ, Olofsson A, Levy D, Ranck JL (1997) Bio-Beads: an efficient strategy for two-dimensional crystallization of membrane proteins. J Struct Biol 118:226–235

Ronzon F, Morandat S, Roux B, Bortolato M (2004) Insertion of a glycosylphosphatidylinosiyol –anchored enzyme into liposomes. J Membrane Biol 197:167–177

Salafsky J, Groves JT, Boxer SG (1996) Architecture and function of membrane proteins in planar supported bilayers: a study with photosynthetic reaction centers. Biochemistry 35:14773–14781

Sennhauser G, Amstutz P, Briand C, Storchenegger O, Gruetter MG (2007) Drug export pathway of multidrug exporter AcrB revealed by DARPin inhibitors. PLoS Biol 5:e7

Sharom FJ, Lehto MT (2002) Glycosylphosphatidylinositol-anchored proteins: structure, function, and cleavage by phosphatidylinositol-specific phospholipase C. Biochem Cell Biol 80:535–549

Silvius JR (1992) Solubilization and Functional Reconstitution of Biomembrane Components. Annu Rev Biophys Biomol Struct 21:323–348

Tamura N, Murakami S, Oyama Y, Ishiguro M, Yamaguchi A (2005) Direct interaction of multidrug efflux transporter AcrB and outer membrane channel TolC detected via site-directed disulfide crosslinking. Biochemistry 44:11115–11121

Trépout S, Mornet S, Benabdelhak H, Ducruix A, Brisson AR, Lambert O (2007) Membrane protein selectively oriented on solid support and reconstituted into a lipid membrane. Langmuir 23:2647–2654

Wenk MR, Alt T, Seelig A, Seelig J (1997) Octyl-β-Dglucopyranoside partitioning into lipid bilayers: thermodynamics of binding and structural changes of the bilayer. Biophys J 72:1719–1731

Yoneyama H, Maseda H, Kamiguchi H, Nakae T (2000) Function of the membrane fusion protein, MexA, of the MexAB-OprM efflux pump in Pseudomonas aeruginosa without an anchoring membrane. J Biol Chem 275:4628–4634